

# 3

## Multi-Electrode Arrays: Enhancing Traditional Methods and Enabling Network Physiology

JAMES WHITSON, DON KUBOTA, KEN SHIMONO, YOUSHENG JIA,  
AND MAKOTO TAKETANI

### Introduction

Early research in the field of multi-electrode arrays (MEAs) was largely concerned with the development of MEA hardware (see Chapter 1 for a review). This research lay the ground work that enabled commercial entities, such as Panasonic (Oka et al., 1999) and Multi Channel Systems (Egert et al., 1998), to develop and manufacture the first MEA-based instruments to be sold in large numbers. Current estimates place the number of instruments sold at over 250 worldwide. The proliferation of these instruments within the electrophysiology community has led to a variety of new applications. This chapter presents a sampling of these applications meant to outline some of the major application categories currently associated with MEAs.

In what follows, MEA applications are divided into two broad categories: experiments that can be performed with traditional non-MEA instrumentation but are enhanced by the use of MEAs; and experiments that can only be performed using MEAs because they depend upon one or more of their unique characteristics. Within each of these broad categories a variety of protocols, tissue types, tissue preparations, and measurements is presented. The examples are largely drawn from users of the Panasonic MED64 System due to the authors' unique access to these researchers; however, the broad outline offered here should apply to users of other MEA instrumentation as well.

### 3.1 Enhanced Traditional Methods

Traditional slice electrophysiology employs individually implanted glass or metal electrodes to stimulate and record from brain slice tissue. These experiments typically measure spikes, evoked field potentials, or spontaneous field potentials under either static or interface conditions within a slice recording chamber. The tissue samples used in these experiments may derive from a wide variety of brain regions, and they may derive from adult animals for acute testing (lasting hours) or from very young animals for culture testing (lasting days or even weeks).

Over the years, improvements made to MEA hardware have enabled them to perform the same types of experiments as traditional electrophysiology instrumentation. The first MEAs developed in the 1970s were used to record spiking behavior in both acute and culture tissue preparations (Gross et al., 1977; Gross, 1979). Later improvements would add stimulation capabilities (Jobling et al., 1981). However, the relatively high impedance of the early electrodes did not permit the recording of field potentials. The first MEA field potential recordings were achieved by Novak and Wheeler (1988), who succeeded in recording field potentials for two to four hours before the electrodes failed. This early success lay the groundwork for the later development of improved electrodes with the sort of fidelity and survival time required to implement all the major categories of traditional slice electrophysiology (Oka, 1999). However, although modern MEAs can in general perform all the major types of traditional experiments, they are not always the best choice for a particular application.

Determining MEA applicability requires careful consideration of their specific strengths and weaknesses. Ignoring for the moment their potential to enable entirely new types of experiments, their major strengths from a traditional perspective include: (1) the ability to gather data from multiple sites in parallel as if running multiple experiments in a single slice; (2) the ability to change stimulation and recording sites very quickly among those available in the array; (3) the ability to easily set up “within-slice” controls by taking advantage of the many available electrodes; and (4) avoiding the need to place multiple electrodes individually by hand. Limitations include: (1) in most cases, smaller amplitude recordings as compared to traditional instrumentation because the electrodes are not inserted inside the tissue; (2) the electrodes cannot be moved independently because they are arranged in a fixed pattern; and (3) the sensitivity to fluid level fluctuations under “interface” conditions is often greater than that seen with traditional instrumentation.

The sample applications that follow illustrate the use of MEAs for each of three major categories of traditional electrophysiology: spike recording, evoked field potentials, and spontaneous field potentials. They also illustrate the use of MEAs for the study of a variety of different tissue types and preparations, and many demonstrate drug testing. For each application shown, the reasoning behind the choice of MEA is discussed.

### *3.1.1 Spike Recording*

#### Acute Hypothalamic Slices

The hypothalamus is a key brain structure known to regulate a variety of autonomic and hormonal functions. As such, it is the focus of research aimed at understanding and treating a variety of diseases. Some researchers are pursuing the study of hypothalamus using MEAs (Welsh et al. 1995; Honma et al. 1998). Given that the hypothalamus contains a variety of nuclei, a single slice placed on top of an MEA affords researchers easy access to multiple nuclei (Figure 3.1), enabling them to stimulate and record from multiple regions within a single slice. For spike recording experiments, this means the researcher can record more spiking cells

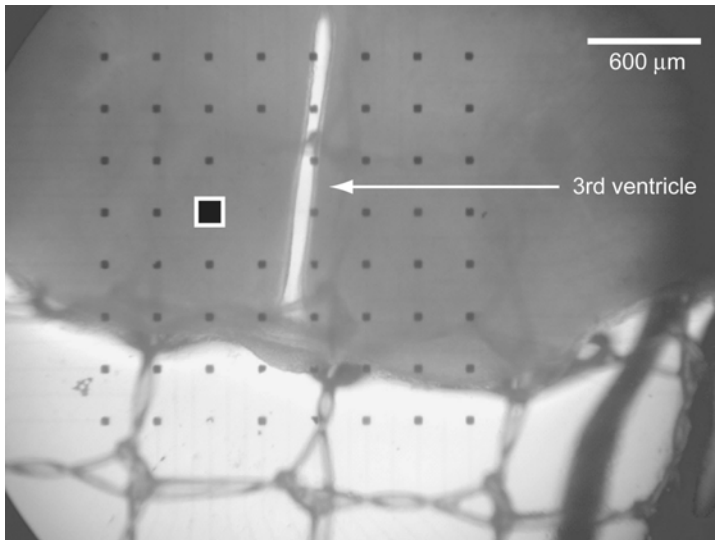


FIGURE 3.1. Micrograph of a coronal rat brain slice, bregma  $-3.14\text{mm}$ . A 64-electrode array covers the periventricular nucleus, the arcuate nucleus, the median eminence, and the part of the ventro-medial and the dorso-medial hypothalamic nucleus. The white arrow indicates the third ventricle, and the black-filled square the site of the electrode used for stimulation.

per slice, and he or she can easily discover and record from different cell types producing different behaviors in parallel.

An example of just such a case is provided by a recent hypothalamic obesity drug study (unpublished results, Jia, 2004\*). Figure 3.2 shows a rat hypothalamus slice placed on top of an  $8 \times 8$  multi-electrode array and several single unit recordings that were taken at the same time from different indicated locations in the slice. After recording a stable spike rate baseline for each of the units,  $0.1 \mu\text{M}$  Ghrelin was added to the bath. Some units reacted with an increase in firing rate, and others instead decreased their firing rate. Previous work in the hypothalamus predicts this effect and attributes it to different cell types. These expected but opposite responses serve as a within-slice control condition helping to validate the results gathered from each slice.

Hypothalamic slices on MEAs have proven effective for testing obesity drugs. Figure 3.3 compares the results obtained with 5-HT and d-FEN (the “Fen” half of the weight loss drug known commercially as “Fen-Phen”). The results show that the two compounds have similar effects as expected: both are known to suppress appetite in behavioral studies. For this application the MEA offered key advantages. On average, four to five units were recorded per slice without the need to implant

\* Data courtesy Dr. Yousheng Jia, Tensor Biosciences, Irvine, CA 92612, USA.

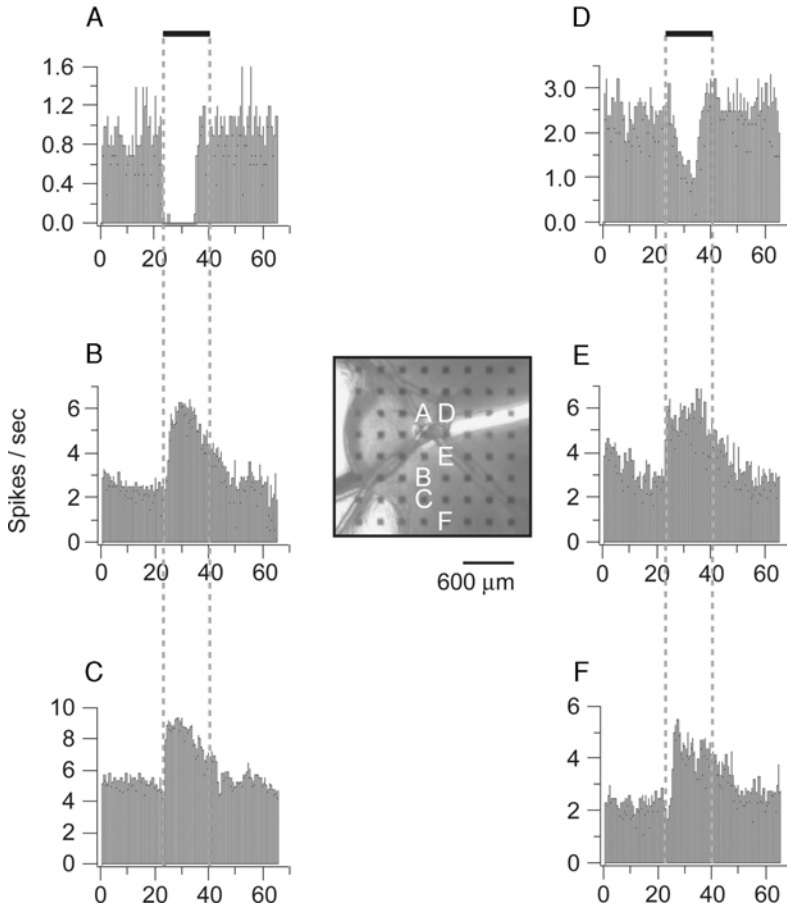


FIGURE 3.2. A hypothalamic slice with multiple spiking unit recordings from a MEA. The central image is a micrograph taken of a hypothalamic slice on top of an array of 64 electrodes arranged in an  $8 \times 8$  grid. Each of the small black squares is an electrode. Six different electrodes produced spiking single units. These are indicated on the micrograph in white letters A–F. Each of the six electrodes has a correspondingly lettered spike frequency plot (spikes/second) indicating the change in spiking behavior observed during baseline, Ghrelin application, and washout. (Courtesy of Tensor Biosciences.)

and move multiple electrodes by hand, as would be necessary to achieve this many unit recordings with traditional instrumentation. And the recording of cells with opposite drug reactions helped to validate the results obtained from each slice.

#### Dissociated Dorsal Root Ganglia Cell Cultures

In humans, sensory axons innervating the torso and limbs originate from the dorsal root ganglia (DRG). Its cells serve to relay sensory information from muscles, skin, and joints to the spinal cord. Much of the research in this area concerns the treatment

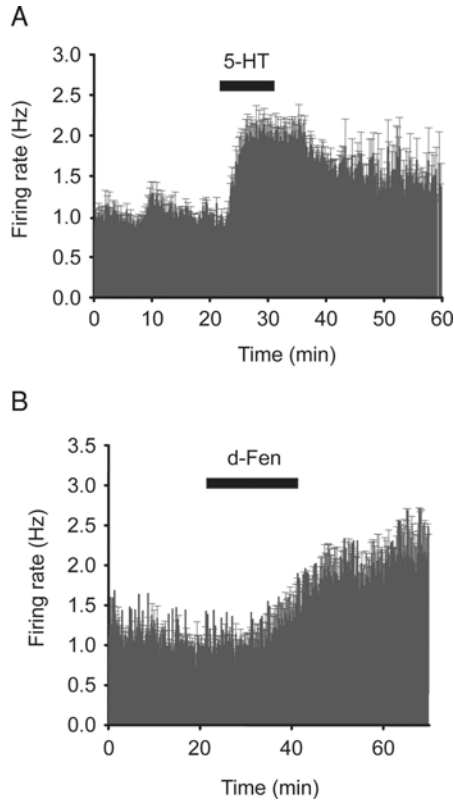


FIGURE 3.3. The excitatory effect of 5-HT and d-FEN on single units in rat arcuate nucleus. (A) The spiking rate of multiple single units is plotted before and after the application 5HT; (B) and also before and after the application of d-FEN. In both case, the horizontal black bar below the drug name indicates the duration of drug application. (Courtesy of Tensor Biosciences.)

of pain. In particular, the inhibition of capsaicin-induced current may provide a basis for reducing capsaicin receptor-mediated nociception (Chen et. al., 2004). Recent work using cultured DRG neurons on a MEA demonstrates the feasibility of studying spiking DRG neurons at multiple sites in parallel.

A MEA with cultured DRG neurons spread broadly across its 64 electrodes is shown in Figure 3.4. Spiking behavior is seen at three of the electrodes after applying 1  $\mu$ M Capsaicin. Here, the primary advantage of the MEA is throughput and labor reduction: one simply spreads the neurons broadly over the array, waits for the culture to mature, and then examines all 64 sites in parallel to find good spiking neurons. Probably not all sites will have neurons worth recording, but even if just a few are found, this approach is still much faster than using traditional instrumentation to search by moving one or more implanted electrodes by hand.

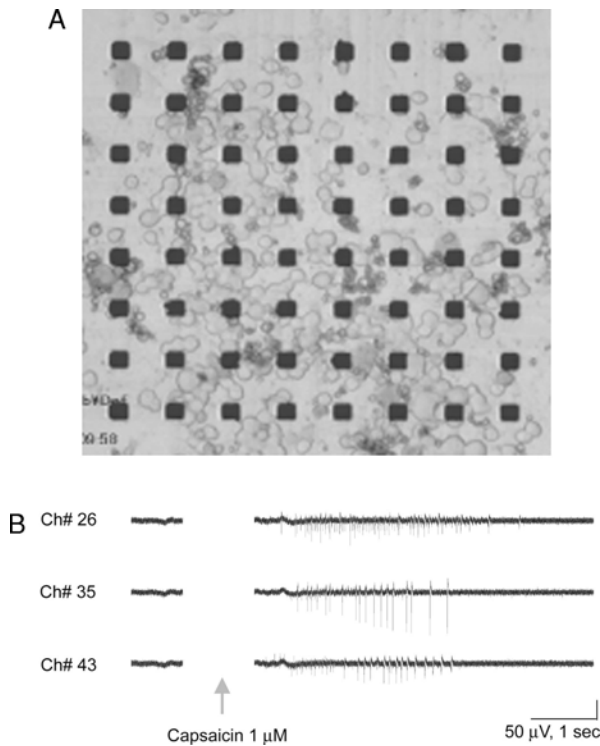


FIGURE 3.4. Cultured DRG neurons showing Capsaicin induced spiking. (A) Micrograph of cultured rat DRG neurons after three days on MED-P515A probe (150  $\mu\text{m}$  spacing). (B) Spontaneous responses were recorded from each electrode. Capsaicin (1  $\mu\text{M}$ ) elicited repetitive spikes for several seconds. (Courtesy of Alpha MED Sciences, Co., Ltd.)

### Co-Cultured Organotypic Septo-Hippocampal Slices

In contrast to the dissociated cell culture of the previous section, the micrograph shown in Figure 3.5 depicts an organotypic co-culture. The tissue slice at the top of the micrograph is a slice taken from a neonatal rat (+9 days), and the slice at the bottom is from the septum (+5 days). In the intact brain, the septum sends cholinergic axonal projections into the hippocampus that are thought to help govern rhythmic activity in the hippocampus. After being co-cultured for 19 days, spike recordings are taken using the two electrodes circled in Figure 3.5.

Figure 3.6 shows how spiking behavior is affected by the application of physostigmine and atropine: the former increases the spike rate over baseline, whereas the latter decreases it. Because physostigmine is a cholinesterase inhibitor and atropine is a muscarinic receptor inhibitor, these results strongly suggest that working cholinergic synapses have formed in the hippocampus due to an influx of septal projections. In other words, *in vivo* septo-hippocampal anatomy is being

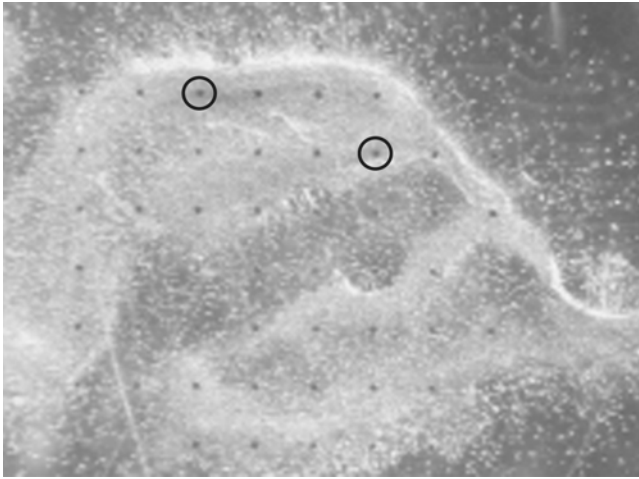


FIGURE 3.5. Micrograph of septo-hippocampal co-culture. Septum slices (bottom half, from 5-day-old rats) were co-cultured with hippocampal slices (upper half, from 9 day-old rats) on the Panasonic MED-P545 probes for 19 days (450  $\mu\text{m}$  interelectrode distance). Spontaneous activity was measured from the two electrodes shown circled.

mimicked by the co-culture. The use of a MEA with transparent wiring here helps make tracking the health of the culture visually very easy.

### 3.1.2 *Evoked Field Potentials*

#### Acute Hippocampal Slices

The hippocampus is a key player in the formation of memories. As such, it is the focus of intense research aimed at treating Alzheimer's and other memory-related disorders. It is also very well suited for slice studies owing to the planar organization of projections among its subfields. Figure 3.7 summarizes its major projections systems and the regions of interest to electrophysiologists. For each subfield, there is a different preferred method of stimulation and a different expected response. The study of these responses can reveal much about the mechanisms underlying the function of a compound.

A number of researchers are pursuing the study of the hippocampus with MEAs (Novak and Wheeler, 1988; Egert et al. 1998; Shimono et al. 2000). Figure 3.8 shows a case where an AMPA reuptake inhibitor is applied to a hippocampal slice, and altered responses are seen under four different conditions at three locations in the slice (two different stimulation patterns are applied to CA1). Although these experiments could also be performed with traditional instrumentation, there are a few key advantages gained through the use of MEAs here. There is increased throughput owing to the ability to stimulate and record from multiple sites, and the different responses expected in the various regions act as within-slice controls that help validate the viability of the slice and the experimental conditions.

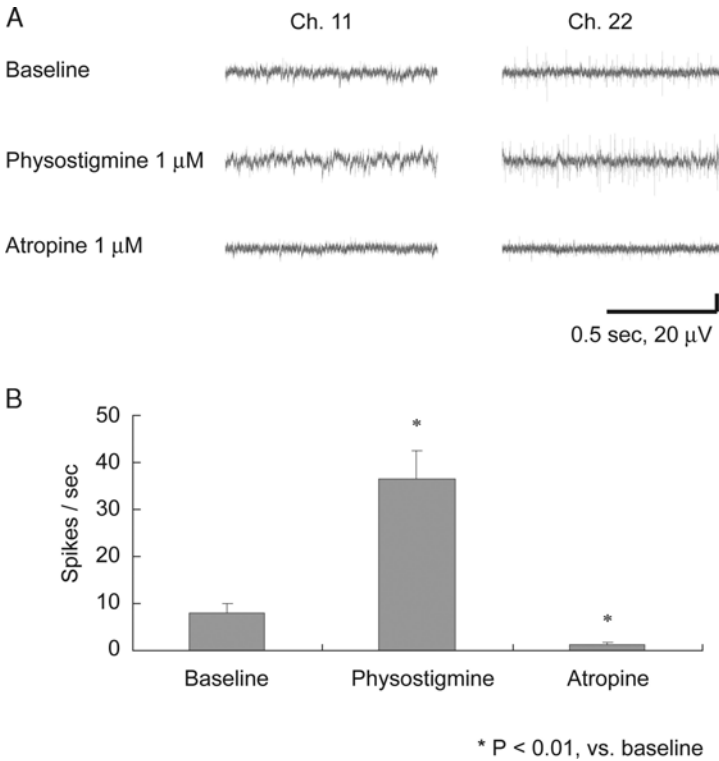


FIGURE 3.6. Evaluation of drug effect on co-cultured septo-hippocampal slice. (A) Physostigmine 1  $\mu\text{M}$ , a cholinesterase inhibitor, increased activities in both CA1 and CA3. Atropine 1  $\mu\text{M}$ , a muscarinic receptor antagonist, blocked activity. (B) Quantification of the effects of physostigmine and atropine. Results are means  $\pm$  SEM of data obtained in 2 slices, 4 recording electrodes in hippocampus area in each slice.

### Acute Spinal Cord Slices

Research focused on the spinal cord concerns both functional questions as well as treatments for various health problems, among them paralysis and pain. Several studies of spinal cord slices employ MEAs (Tschertter et al., 2001; Streit et al., 2001; Darbon et al., 2004; Legrand et al., 2004). Figure 3.9 demonstrates the viability of using an MEA to study spinal cord tissue. A MEA is placed on the dorsal horn of a rat spinal cord slice. Upon stimulation, the expected responses are seen among the electrodes adjacent to the stimulation sites.

### Acute Heart Slices

Among electrophysiologists, heart research is largely concerned with the oscillatory behavior of the neurons that control heart muscle contractions. This work can lead to a better understanding of heart function and treatments for diseases such



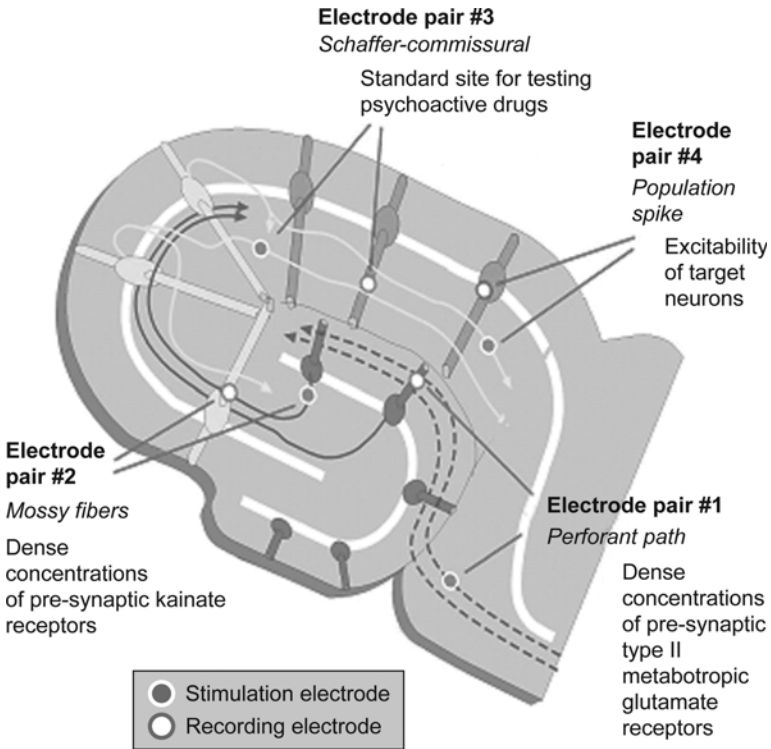


FIGURE 3.7. Stimulating and recording sites on hippocampal tri-synaptic circuit. Axonal projections travel among the subregions. The order of the projections is as follows: entorhinal cortex to DG (electrode pair #1) to CA3 (electrode pair #2) to CA1 (electrode pair #3) to subiculum (electrode pair #4). For each of the regions shown with a stimulation and recording electrode pair, there is a characteristic response expected for a particular stimulation pattern. (Courtesy of Tensor Biosciences.)

as arrhythmia. A number of researchers employ MEAs in this field (Feld et al., 2002; Lu et al., 2004). Figure 3.10 demonstrates the use of a MEA to study a drug effect on heart tissue. Here ventricular tissue is placed on top of the array and evoked responses are recorded using 100 mM Quinidine during baseline, washin, and washout. The drug increases the latency and duration of the evoked action potentials.

### 3.1.3 Spontaneous Field Potentials

#### Acute Hippocampal Slice Oscillations

Rhythmic oscillations are a fundamental feature of brain physiology. Indeed, disruptions to brain wave activity (electroencephalograms) have been used clinically

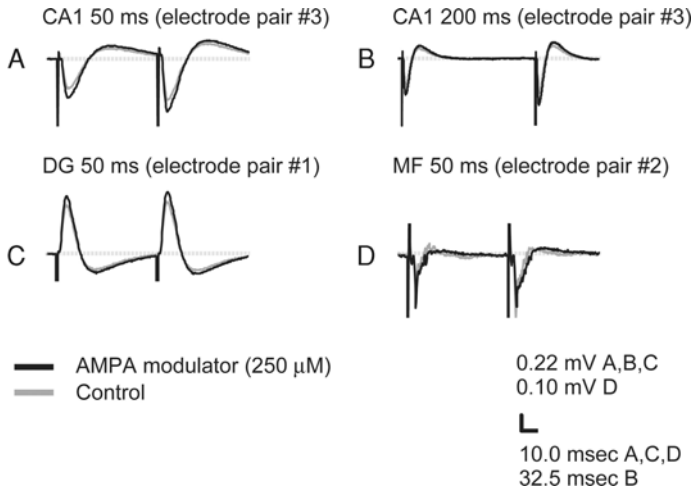


FIGURE 3.8. Drug effects on paired-pulse field EPSPs in various areas of rat hippocampus. The gray trace is before and black trace is after the application of a 250  $\mu$ M AMPA modulator. (A) Shows response from CA1 for a 50 msec paired-pulse stimulation; (B) Shows response from CA1 for a 200 ms paired-pulse stimulation; (C) Shows response from DG for a 50 msec paired-pulse stimulation; (D) Shows response from CA3 for a 50 msec paired-pulse stimulation. (Courtesy of Tensor Biosciences.)

for decades to diagnose brain damage and disease *in vivo*. Now researchers are using hippocampal slices and MEAs to study this oscillatory behavior *in vitro* (Shimono et al., 2000; Paulsen, 2003). In an intact brain, cholinergic inputs from the septum to the hippocampus govern hippocampal rhythmic activity. In a slice, carbachol can be used to artificially induce cholinergic rhythms in the hippocampus. Figure 3.11 shows the varied effects of carbachol within each subfield of the hippocampus. A steady beta rhythm (10 to 30 Hz) is seen most prominently among the apical dendrites of CA1 and CA3. In Figure 3.12, using a larger MEA to record from a broader area reveals the varied effects of carbachol for two different anatomical structures: the rhythmic oscillations of entorhinal cortex are found to be higher in frequency than those of the hippocampus. Notice that the use of MEAs here enables the easy observation of rhythms at multiple slice locations in parallel.

### Synchronized Cardiac Muscle and Stem Cell Culture Activity

Stem cell research holds great potential for improving both our understanding of brain function and the treatment options for diseases such as Parkinson's. Some stem cell researchers are turning to MEAs for their electrophysiology work (unpublished results, Kodama et al., 2004). Figure 3.13 provides an example: a MEA is shown with a partition dividing its left and right sides. Cultured neonatal cardiac

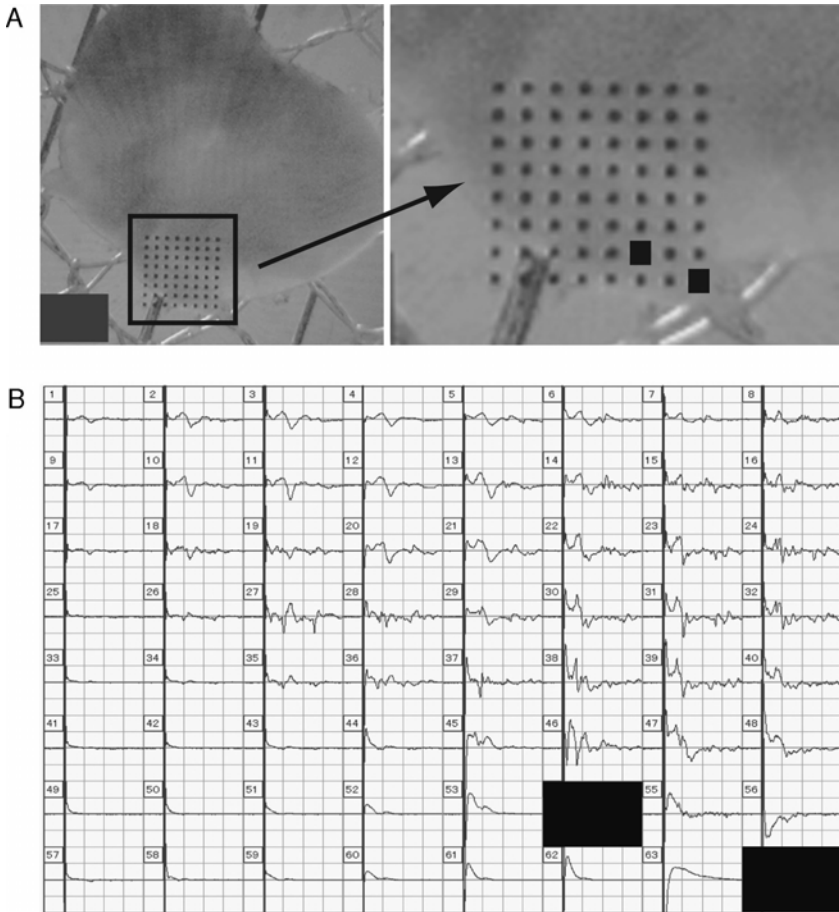


FIGURE 3.9. Evoked response from rat spinal cord slice. (A) Micrographs of a slice from rat spinal cord placed on a Panasonic MED-P210A probe (100  $\mu\text{m}$  inter-polar distance) and centered on dorsal horn (left) and close-up of outlined region (right). (B) Bipolar stimulation is delivered using electrodes located at the edge of dorsal root (marked with large black squares). (Courtesy of Alpha MED Sciences Co., Ltd.)

muscle cells have been grown on the left side, and embryonic stem cell derived cardiac muscle cells have been grown on the right side. Part A of Figure 3.14 shows the activity obtained from the separated cells. Both sides are clearly alive and active. Part B of Figure 3.14 shows that after removing the partition and waiting for three days, synchronous activities appear among the stem cells on the right side. This study suggests that cardiac muscle cells derived from embryonic stem cells can create “electrical syncytium” with intact cardiac muscle cells. Similar work has also been done by Egashira et al. (2004). The use of a MEA for this application makes it quite easy to locate sites of synchronized activity on each side of the partition line.

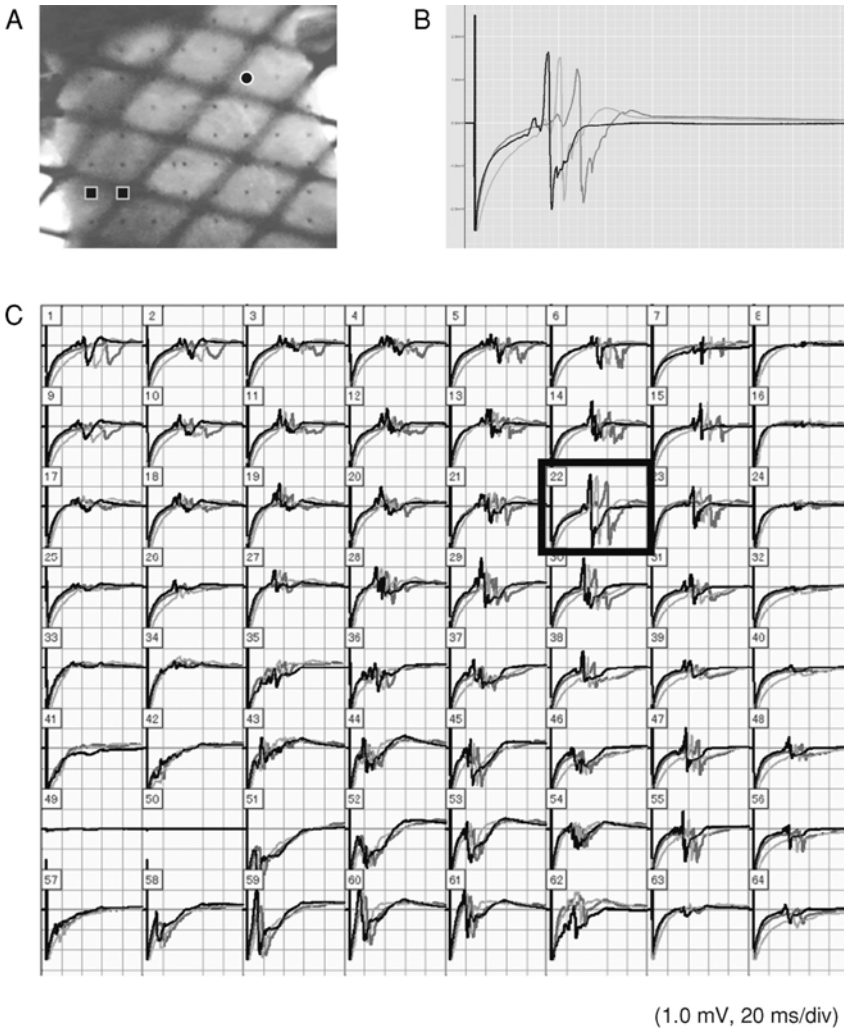


FIGURE 3.10. Drug effect on acute ventricular muscle slice. (A) Micrograph of adult rat left ventricular muscle slice with 250  $\mu\text{m}$  thickness. The two filled black squares near the lower left denote the stimulation sites while the black circle near the upper right the recording site of interest—electrode 22. (B) Pacing response at electrode 22 evoked by 100  $\mu\text{A}$  electric stimulation to the two electrodes: the leftmost black trace is without drug, the rightmost medium gray trace is with drug, and the middle light gray trace is washout. In the presence of 100  $\mu\text{M}$  Quinidine, the latency and the duration of the action potential were prolonged. (C) The responses from all 64 electrodes with electrode 22 outlined in black. (Courtesy of Alpha-MED Sciences, Co., Ltd.)

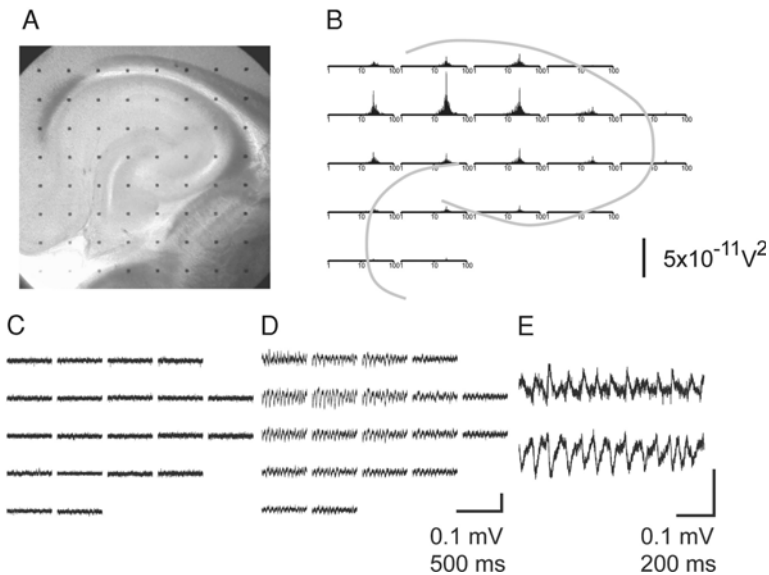


FIGURE 3.11. Distribution of carbachol-induced beta waves within the hippocampus. (A) Micrograph of hippocampal slice on an MEA. (B) Spectra of carbachol-induced spontaneous activity at 20 electrodes on a logarithmic scale from 1 to 100 Hz. Activity is seen in the 10 to 30 Hz frequency range, primarily in apical dendrites of fields CA1 and CA3 (calibration bar:  $5 \times 10^{-11} \text{V}^2$ ). (C) Activity in baseline conditions. (D) Activity measured after infusion of 50  $\mu\text{M}$  carbachol (calibration bars for (C) and (D): 0.1 mV; 500 msec). (E) Reversal of polarity across the cell body layer of field CA1 (calibration bars: 0.1 mV; 250 msec). (Figure copyrighted 2000 by the Society for Neuroscience.)

### 3.1.4 Summary of MEA Advantages for Traditional Physiology

MEAs enable the performance of many new types of experiments that cannot be performed at all with traditional instrumentation (see Section 3.2). However, as a potential replacement for traditional instrumentation in the performance of traditional experiments, MEAs, like any new tool, have their strengths and weaknesses.

The potential advantages of MEAs over traditional instrumentation for various combinations of tissue preparations and slice chamber conditions are summarized in Table 3.1. For each combination, a list of the potential advantages is given. The lists use the terms: “site sel” which refers to speeding up the selection of stimulation and recording sites that yield stable baseline responses; “parallelism” refers to the potential to essentially run multiple traditional experiments in one slice; and “sterile” refers to the potential to increase the sterility of slice conditions, which is only important for cultures, by growing them directly on MEAs, storing them under closed conditions, and avoiding repeated electrode insertions and extractions. Next to the list items are plus, minus, and equal signs indicating

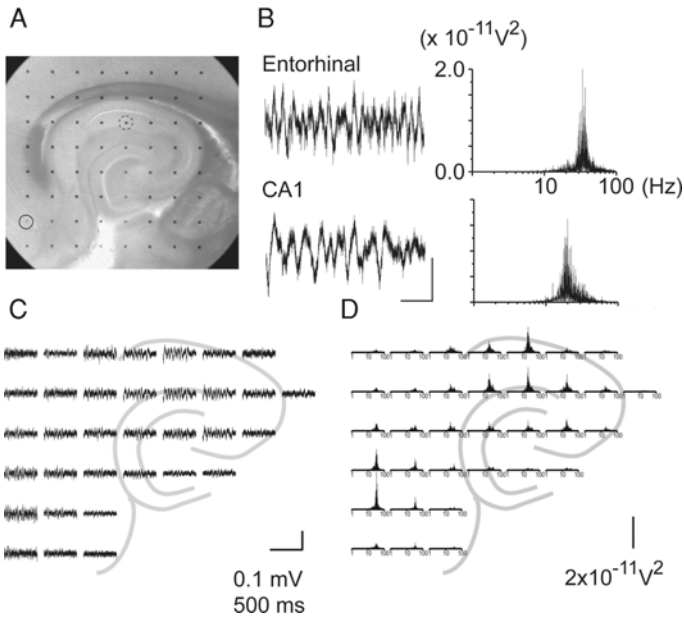


FIGURE 3.12. Two distinct carbachol-induced rhythms in hippocampus and cortex. (A) Micrograph of a cortico-hippocampal slice on a broad array. The solid circle in the lower left denotes an entorhinal cortex electrode, the dotted circle in the upper middle a CA1 electrode. (B) Sample activity in response to infusion of carbachol ( $50 \mu\text{M}$ ) from the selected electrodes in entorhinal cortex and field CA1 (left) and power spectra for recordings over 3 seconds at these two sites (right). (Left calibration bars:  $50 \mu\text{V}$ , 100 msec; right charts share the same calibration.) Although field CA1 exhibits betalike rhythm centered around 20 Hz, carbachol elicits higher frequency (35 to 40 Hz) activity in entorhinal cortex (top right spectrum). (C) Distribution of representative activity in the slice (calibration bars: 0.1 mV, 500 msec). (D) Distribution of low-pass (0 to 100 Hz) filtered power spectra in the slice (calibration bar:  $2 \times 10^{-11} \text{V}^2$ ). (Figure copyrighted 2000 by the Society for Neuroscience.)

when there is an advantage, disadvantage, or no gain for MEAs over traditional setups. A plus/minus combination means the results obtained will depend on the specific application. An equal/minus combination means they are either equal or there are disadvantages to using MEAs over traditional instrumentation.

A review of the table entries reveals that some combinations of experimental conditions and tissue preparations more clearly favor the use of MEAs than others. The most potentially advantageous combination is “dissociated cell cultures” and “static and submerged” conditions, where one would expect faster selection of stable recording sites, many parallel experiments (in the best case one per electrode), and increased culture sterility if desired. The least potentially advantageous combination is “acute slices” and “perfused and interface” conditions. Here, the careful tuning of the fluid level that may be necessary to achieve a stable baseline

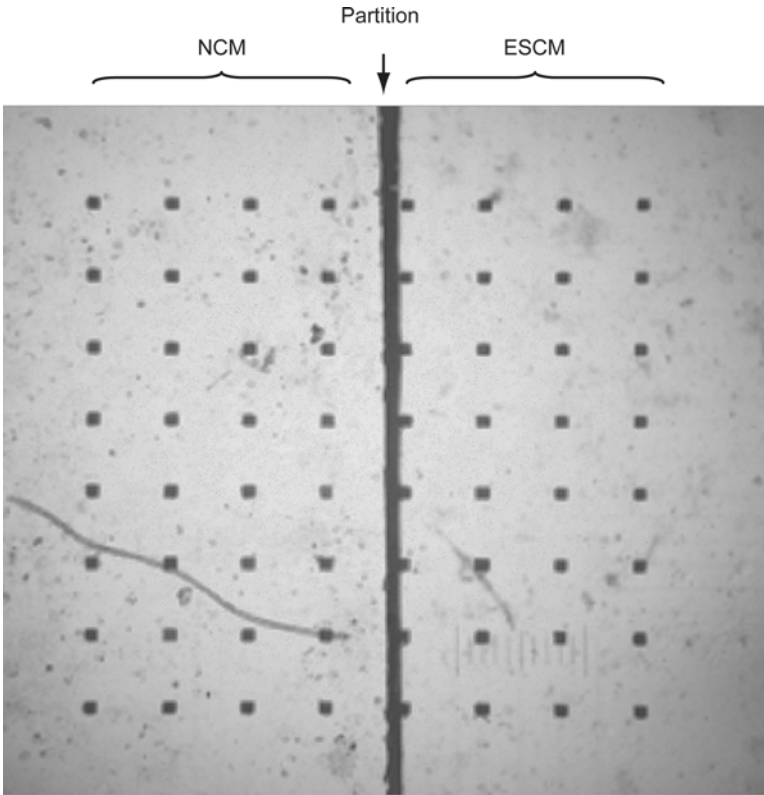


FIGURE 3.13. Detailed view of the microelectrode array area containing cardiac muscle cells and embryonic stem cells. Left side: neonatal cardiac muscle cells (NCM). Right side: embryonic stem cell cardiac muscle cells (ESCM). A physical partition divides the two sides at the beginning of the experiment.

under interface conditions can slow the site selection process; however, the impact of this issue depends mostly on the skill of the practitioner, so with training it can be mitigated.

At the risk of stating the obvious, the following conditions should be met by an experiment before undertaking it with MEAs.

- Because it is impossible to move any of the electrodes independently, one needs an array size and shape that conforms to the stimulation and recording electrode placements needed for the experiment;
- The speed advantages offered by MEAs increase with decreasing placement accuracy requirements, because there is an inherent tradeoff between the time taken to place a slice on an array and placement accuracy;
- Given that the recordings made with a MEA often have smaller response amplitude than traditional instrumentation, it is important to make sure that the signal-to-noise ratio is sufficient to gather viable data.

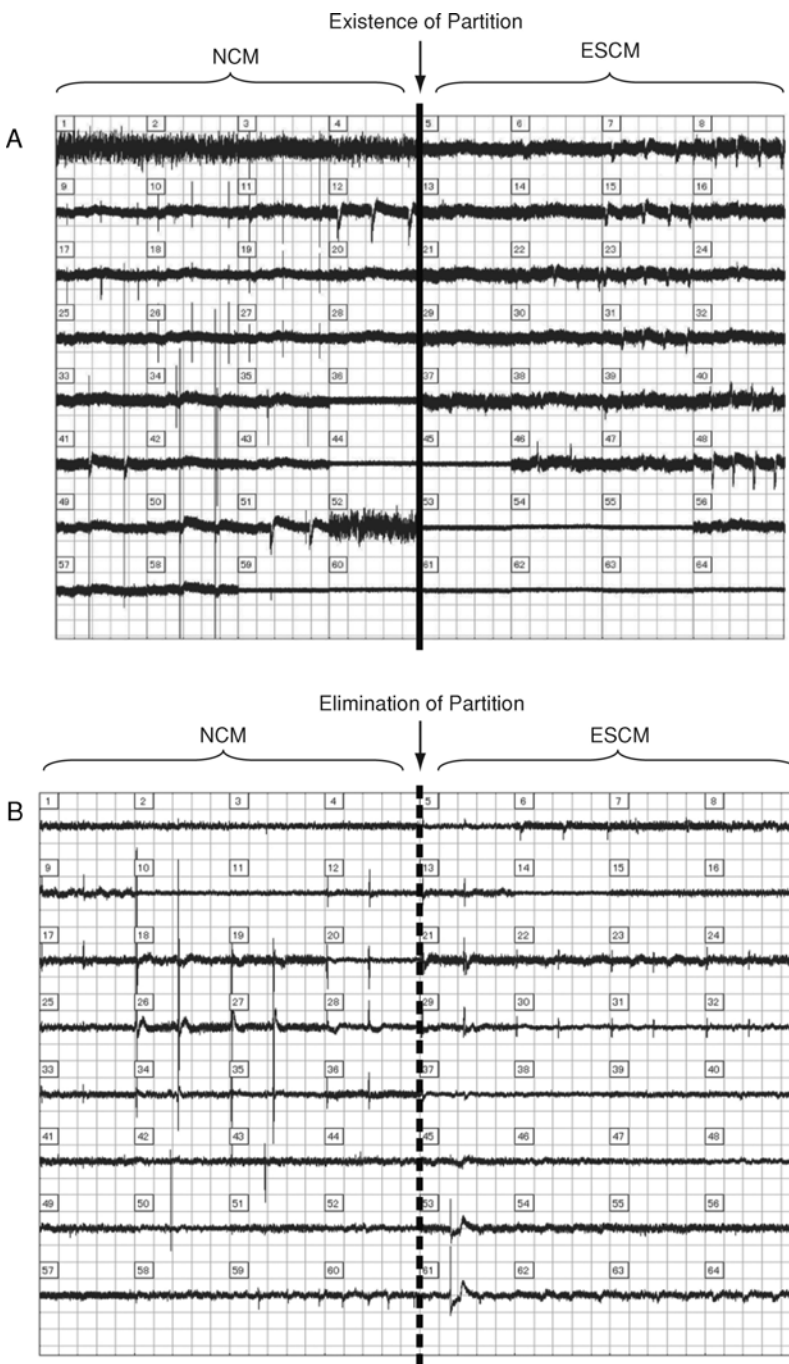


FIGURE 3.14. Activity changes of cardiac muscle cells derived from embryonic stem cells. (A) Spontaneous field potentials from 64 sites in the presence of partition. Independent activities observed in both left and right side cultured cells. (B) Electrical responses from 64 sites in the absence of partition. (Courtesy of Drs. Lee and Kodama, Nagoya University, Japan.)



TABLE 3.1. Potential MEA advantages over traditional setups.

	Acute slices	Dissociated cell cultures	Organotypic cultures
Perfused and submerged	+ site sel +/- parallelism	No data	No data
Perfused and interface	= /- site sel +/- parallelism	No data	No data
Static and submerged	+ site sel +/- parallelism	+ site sel + parallelism + sterile	+ site sel +/-parallelism + sterile
Static and interface	+ site sel +/- parallelism	No data	No data

## 3.2 New Methods: Network Physiology

This section presents a sampling of MEA applications that are difficult or impossible to perform using traditional instrumentation. These applications rely upon various unique characteristics of MEAs and are typically concerned with the study of network-level phenomena. Many make use of the two-dimensional (2-D) nature of the MEA grid to measure network phenomena in new ways, such as 2-D current source density and phase maps. Others use MEAs to grow networks in culture form directly on the multi-electrode array, which enables stimulation and recording from specific locations in the slice day after day; with traditional culture preparations on membranes the electrodes cannot easily be maintained in specific locations for long periods.

### 3.2.1 Two-Dimensional Current Source Density Analysis

#### Discovering Functional Anatomy in the Hippocampus

For decades there has been a great deal of interest in modeling the functional behavior of the hippocampal trisynaptic circuit (Marr 1971; McNaughton and Morris, 1987; Treves and Rolls, 1992; Jarrard, 1993; O'Keefe and Recce, 1993; Buzsaki and Chrobak, 1995; Muller, 1996; Eichenbaum, 1997; Nadel and Moscovitch, 1997; Squire and Zola, 1998; Tulving and Markowitsch, 1998; Lisman, 1999). These efforts have been aided by traditional anatomical and physiological studies that have revealed a great deal about its various components. However, without 2-D recordings of activity patterns using many electrodes, it is difficult to directly determine the extent and pattern of activity propagation across large sections of tissue. In many cases, modelers have had to deduce these properties from indirect evidence.

Work by Shimono et al. (2002) shown in Figure 3.15 demonstrates how an MEA can be employed to reveal the functional anatomy of a region: here axonal inputs to the apical dendrites of the CA1 region are stimulated at various points along the proximal-distal axis. 2-D current source density (2-D-CSD) analysis shows where current sinks develop in response to stimulation at each location. A cumulative analysis of these activity patterns (Figure 3.16) reveals that inputs to CA1 at different levels along the proximal-distal axis have varying levels of

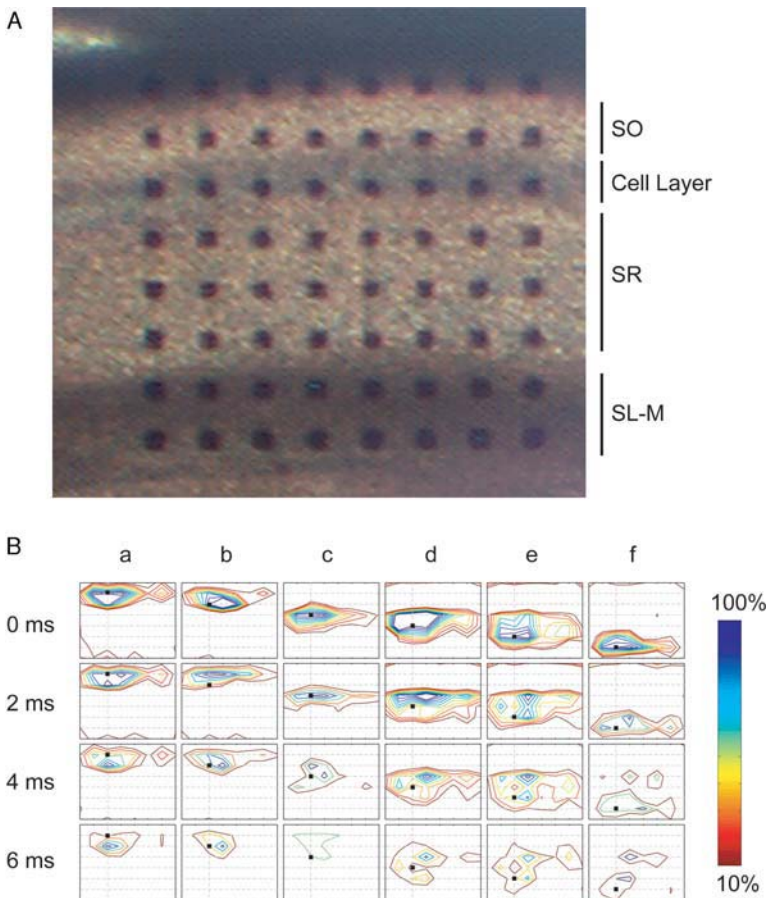


FIGURE 3.15. Computed current sinks shifted along the proximo-distal axis of the CA1 region. (A) Micrograph of a hippocampal slice placed on the microelectrode array with inter-electrode spacing of  $100\ \mu\text{m}$  and centered on apical region of field CA1. (B) The current sinks evoked by stimulation in stratum oriens (second row of the array) are shown in column a. The current sinks evoked in the cell layer—third row of the array—are shown in column b. The current sinks evoked in the stratum radiatum (fourth, fifth, and sixth rows of the array) are shown in columns c, d, and e. The current sinks evoked by the stimulation in the stratum lacunosum/moleculare (seventh row of the array) are shown in column f. In each contour map the filled black square denotes the site of the stimulation electrode. (Reprinted from Shimono et al., 2002, with permission from Elsevier.)

influence on the apical dendritic field: the more distal stimulations were found to be broader than the proximal ones, suggesting the existence of proximally directed collaterals. The lateral influence of the projections, moving parallel to the cell body layer, was essentially bandlike, suggesting that CA1 pyramidal cells are activated in a largely uniform way by these inputs. Note that these results could not be obtained without the use of a 2-D MEA to enable calculation of 2-D current source densities.

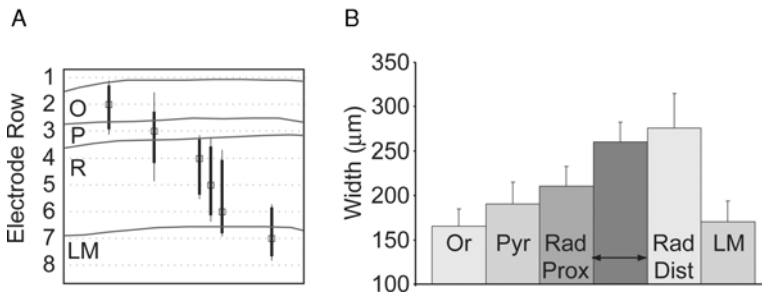


FIGURE 3.16. Statistical analysis of normalized current sinks along the proximo-distal axis. A) micrograph depicting typical electrode placement relative to slice. Single rows of electrodes provide coverage of laminar regions s. oriens, s. pyramidale, and s. lacunosum-moleculare, while three rows span the proximo-distal expanse of s. radiatum. Stimulation by electrodes in each of these rows, shown by black boxes (not drawn to scale), results in sinks whose average proximal and distal extents are shown by thick black bars. Thin black bars represent standard deviations. Results for regions s. oriens through s. lacunosum-moleculare proceed left to right to allow side by side comparison and do not correspond to electrode columns. B) Average proximo-distal widths of current sinks by lamina. Sinks within s. oriens are relatively small, remaining constrained by the cell boundary layer. As stimulation proceeds apically, sinks increase in width. (Reprinted Shimono et al., 2002, with permission from Elsevier.)

The work discussed above employed the technique known as current source density analysis. Through a mathematical transformation of field potential data (Nicholson and Freeman, 1975; Nicholson and Llinas, 1975), an estimate of current source densities can be derived. When the transform is extended to operate on MEA-acquired 2-D field potential data (Shimono et al., 2000), a clear picture of where high and low concentrations of currents into and out of neuronal regions is revealed. If this technique is applied to every timeslice of recorded data, dynamic network-level phenomena become apparent. In short, 2-D-CSD analysis is an example of a new class of tools created to help interpret two-dimensional data and will increase our understanding of the underlying computations of neuronal circuits. The next two subsections introduce other efforts that employ this tool.

### Rhythmic Oscillations in the Hippocampus

Previously, MEAs were shown to add value to the study of rhythmic oscillations in the hippocampus by enabling the easy observation of carbachol induced rhythms at multiple sites in parallel (see Section 3.1.3). However, the spectral analysis of the data gathered across these sites was performed independently per site. The results shown in Figure 3.17 contain a series of 2-D-CSD analyses that can only be performed by combining the readings obtained across a 2-D matrix of equally spaced electrodes. The series reveals the pattern current sources and sinks that emerge as a result of carbachol-induced rhythmic oscillations.

From an arbitrarily chosen starting point, a sink appears in the apical dendrites of the border between fields CA3 and CA1, with an associated source across the

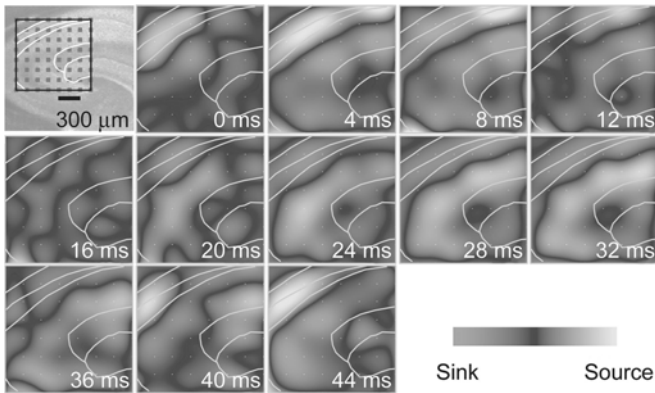


FIGURE 3.17. Current source density analyses of carbachol-induced activity in hippocampus. Each frame shows the instantaneous computed current source density in the region of the electrode array. Taken together they reveal a repeating pattern of sink/source formation across the region. (Figure copyrighted 2000 by the Society for Neuroscience.)

cell boundary layer in the basal dendrites. Within a few milliseconds, an additional focal sink has appeared in apical CA1 with a corresponding basal source. The fields merge and intensify, then dissipate after about 12 msec. After a brief interim during which activity is not distinguished from background, a source appears in the apical dendrites at about 20 msec, with a corresponding sink in the basal dendrites. These expand and intensify before dissipating by roughly 20 msec later (40 msec), after which an apical sink reappears to reinitiate the cycle. The cycle repeats indefinitely (as indicated in the next figure), with an approximate frequency of 25 Hz.

### Atrial Pacing

Previously a MEA was shown to provide a viable platform for studying evoked responses in heart tissue (Section 3.1.3) however, the 2-D nature of the array was used only to speed up the experiment. In contrast, Figure 3.18 shows a 2-D-CSD analysis of sink/source propagation in response to a stimulation delivered at two electrodes in the center of the slice. A series of snapshots of the activity is shown at 5 msec intervals represent a single cycle of pacing oscillatory activity, which begins with sink formation primarily in the upper left quadrant, replaced by a source in roughly the same location 15 msec later. This kind of analysis requires the MEAs a grid of equally spaced electrodes.

## 3.2.2 Phase Maps of Planar Signal Propagation

### Ventricular Pacing

Another form of 2-D analysis that can be performed using a MEA is a phase map. Figure 3.19 shows a phase map obtained by stimulating ventricular tissue at two

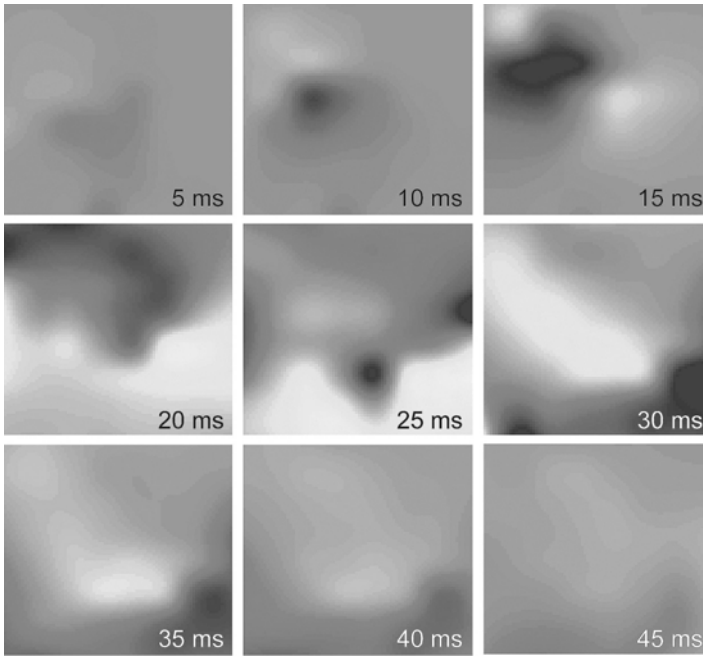


FIGURE 3.18. Propagation of atrial pacing activity. Each time frame shows a computed two-dimensional current source density at a particular time. The times after the stimulation, delivered to the center of the slice, are shown in each panel. Positive potentials are white and negatives are black. (Courtesy of Dr. H.Yeh, Mackay Memorial Hospital, Taiwan.)

stimulation sites (part A) and observing the signal propagation delays (part B). A phase map is a contour plot where the contour lines indicate specific signal propagation delays. In this particular example, the contour lines are plotted at 5 msec intervals. The earliest contour line (5 msec) is closest to the stimulating electrodes in the upper right quadrant of part B. From here, the signal does not propagate across the tissue at a uniform speed; rather, it propagates more quickly through the lower half of the figure than the upper half. This sort of analysis, though possible on a smaller scale (fewer electrodes) using traditional instrumentation, is made very simple over large regions by the use of a MEA.

### Atrial Pacing

Similar to the result just seen for ventricular tissue, signal propagation in atrial tissue can be studied using MEAs. Figure 3.20 shows a case where two sites on the left side of the slice are stimulated (the black squares in part A). The resulting phase map is shown in part B. Unlike the phase map from the ventricular tissue, signals propagate from the stimulation site to the right in a very uniform wavelike manner.

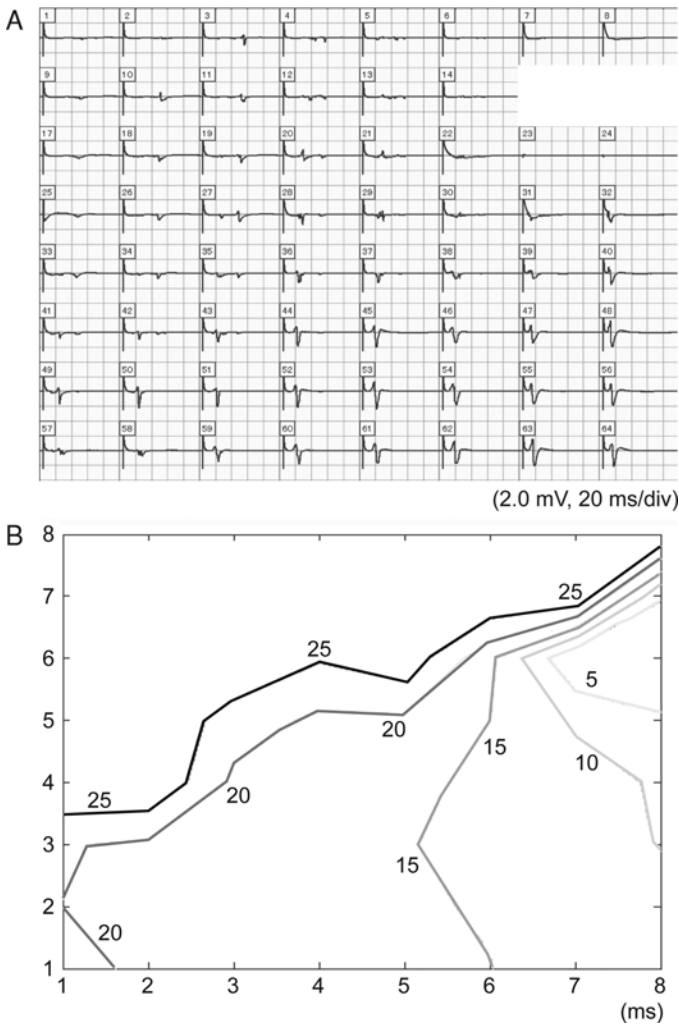


FIGURE 3.19. Evoked response from guinea pig ventricular muscle. (A) Pacing responses (2.0 mV, 20 msec/div) evoked by electrical stimulation (100  $\mu$ A) to the two electrodes on Panasonic MED probe (marked with black rectangles). (B) Phase map of the pacing activity. Each contour shows the latency of the evoked responses from stimulation. (Courtesy of Dr. Tsubone, Graduate School of Agriculture and Life Sciences, University of Tokyo, Japan.)

### 3.2.3 Long-Term Site-Specific Culture Studies

#### LTP Lasting Days in Organotypic Hippocampal Cultures

Organotypic cultures grown directly on the MEA surface were introduced in Section 3.1.1 in the form of septo-hippocampal co-cultures. There, the use of MEAs simplified recording and helped lower the risk of infection; however,

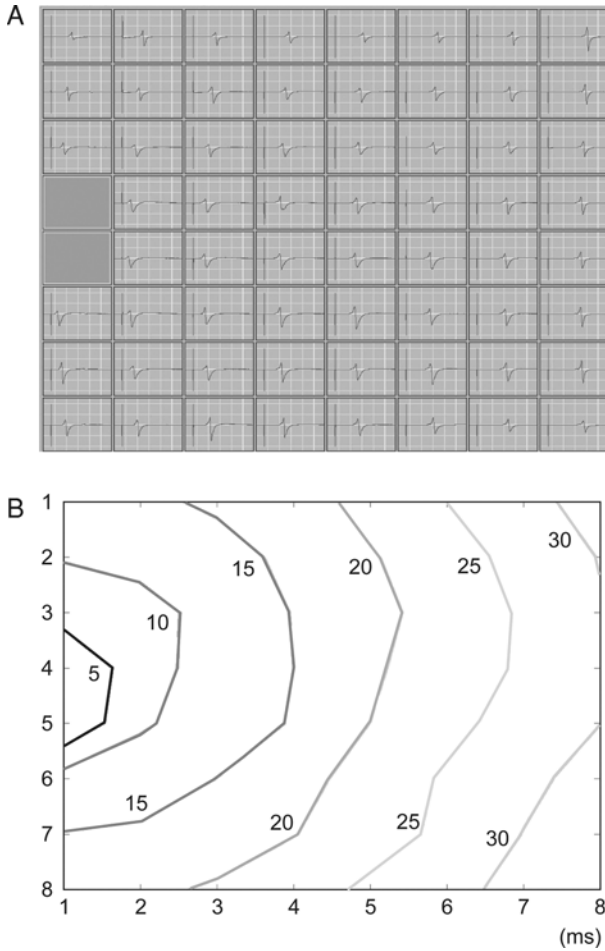


FIGURE 3.20. Primary myocyte culture. (A) Pacing responses were evoked by electric stimulation to the two electrodes on MED probe: the black squares indicate the stimulation sites. (B) Phase map of the pacing activity. Each contour shows the latency in milliseconds of the evoked responses from stimulation. (Courtesy of Drs. Lee and Kodama, Nagoya University, Japan.)

the same results could have been gathered using traditional instrumentation and cultures grown on membranes. Figure 3.21 presents an experiment that can only be performed using a culture grown on a MEA.

The experiment is an LTP study conducted over a two-day period using organotypic hippocampal cultures. Field EPSPs evoked by Schaffer collateral fiber stimulation were recorded in field CA1 before and after tetanus stimulation. High-frequency stimulation intended to potentiate the pathway was delivered during the first hour of the experiment. The maximum amplitude of field

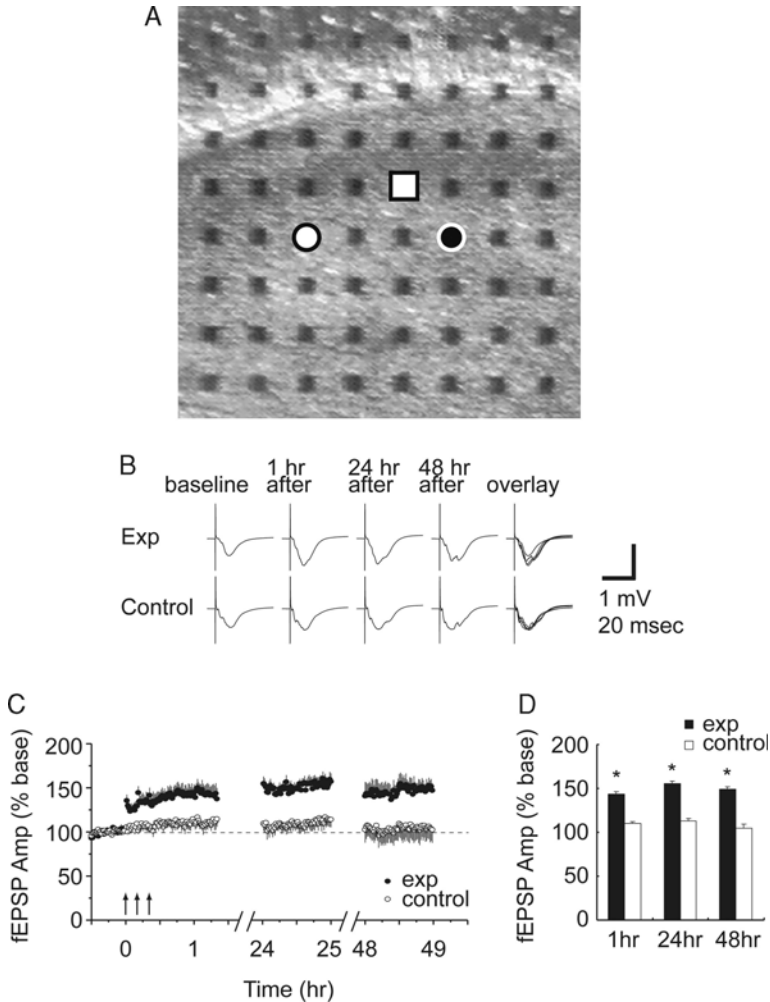


FIGURE 3.21. Long-lasting recording of long-term potentiation in cultured hippocampal slices. (A) Micrograph of a hippocampal slice cultured on an MED probe. The recording electrode is indicated by a white square, and stimulation electrodes are indicated by a white-filled circle (tetanized pathway (exp)) and a black-filled circle (control pathway). (B) Field EPSPs evoked by Schaffer collateral fiber stimulation were recorded in field CA1 before and after tetanus stimulation. (C) Summary graph of long lasting LTP recording. (D) Averaged LTP amplitudes at different intervals.

EPSPs was determined and calculated as a percentage of averaged baseline values (means  $\pm$  S.E.M.,  $n = 8$ ). A statistically significant amount of potentiation was observed throughout the two-day experiment. Figure 3.22 helps to confirm that this effect is indeed LTP by applying a well-known LTP blocker, APV, and observing that LTP is indeed blocked; however, after APV washout it can still be induced.



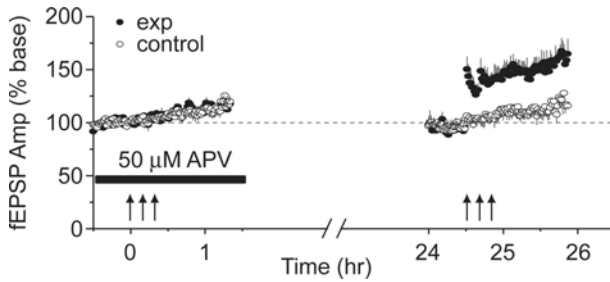


FIGURE 3.22. Reversible blockade of LTP by APV in cultured hippocampal slices. High-frequency stimulation was applied to one pathway (exp) and another unstimulated pathway received low-frequency stimulation (control) in the presence of APV ( $50 \mu\text{M}$ ). Slices were returned to the incubator in culture medium without APV, and were tested the following day. Another high-frequency stimulation was applied to the same pathway and responses measured for another 2 hours. Each point represents the mean  $\pm$  S.E.M. ( $n = 6$ ) of the relative amplitude of fEPSPs in both pathways. Arrows indicate time of high frequency stimulation.

This experiment can only be performed under conditions that enable the same exact axons in a given slice to be stimulated over a period of days, because LTP is a synapse-specific phenomenon. Under normal traditional conditions, if a culture is grown on a membrane, the stimulating and recording electrodes will have to be removed periodically to move the slice into an incubator. It is virtually impossible to reinsert the stimulating electrodes such that they will activate exactly the same axons, day after day. However, if the culture is grown on top of a MEA, the position of the electrodes relative to the tissue is fixed, even when it is placed in an incubator.

### 3.3 Combining MEAs and Fluorescent Microscopy

Another application enabled by MEAs is the combining of multi-electrode electrophysiology and fluorescent microscopy. Microscopy systems offer excellent spatial resolution of activity and can track molecular-level events such as calcium influx into a neuron. MEAs have excellent temporal resolution, and can stimulate slices, triggering events that can be imaged through digital microscopy with a fluorescent dye. MEAs make this possible by allowing a microscope unobstructed access to the slice while at the same time stimulating and recording from the slice. Traditional instrumentation makes this difficult because manipulators and other equipment tend to block or obscure the microscope's access to the slice. A number of researchers are pursuing this methodology (unpublished results, Kilborn et al., 2002<sup>†</sup>). Figure 3.23 shows in part A a micrograph of a hippocampal culture, and

<sup>†</sup> Data courtesy Drs. Ken Shimono, Alpha MED Sciences Co., Ltd., Osaka, Japan; and Karl Kilborn, Intelligent Imaging Innovations, Inc., Santa Monica, CA, USA.

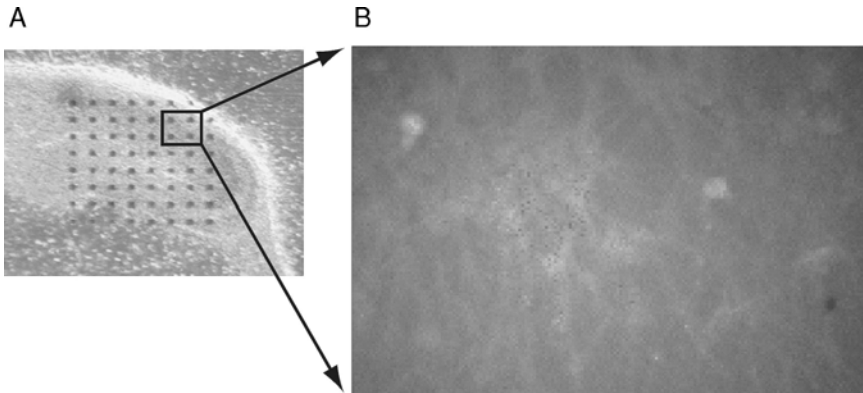


FIGURE 3.23. Micrographs of hippocampal slice and multi-cellular calcium imaging. (A) Hippocampus slice cultured on the MED probe (14 days in culture). (B) Pyramidal layer in the same slice labeled with Fura-2. (Courtesy of Intelligent Imaging Innovations.)

in part B an image of the slice taken with the microscope using a dye for calcium imaging. Figure 3.24 shows in part A the field EPSPs obtained with burst stimulation of the slice. Part B shows the rapid elevation of somatic calcium in dye-loaded cell bodies with the onset of each burst. By one second after each burst, the calcium level returned to near baseline. Early work in this field was done by Jimbo et al. (1993).

### 3.4 The Future: Commercial Drug Discovery

MEAs are making inroads into the pharmaceutical industry. Already, ten out of the top twenty pharmaceutical companies own and use MEA instruments. Most of these are being used to perform traditional types of experiments, often tied to drug safety testing. The enhanced traditional experiments made possible by the use of MEAs fit well with the needs of the drug discovery industry because these tend to increase throughput and reduce labor by simplifying experiments (see Section 3.1).

This is especially true if the hardware and software that are used to run the experiments are also designed to help optimize throughput. Among Panasonic MED64 users in the pharmaceutical industry, having an instrument that makes the selection of different stimulating electrodes very quick and easy has proven very beneficial. Also, the use of wizard-style software (e.g., the “Performer” software from Panasonic) to guide practitioners step by step through traditional protocols is believed to have increased throughput and reduced training time for operators.

Tensor Biosciences has taken these principles a step further with the creation of a drug screening system called the DS-MED. It employs custom software, hardware, and incubators that have all been designed and built to streamline drug screening experiments and increase throughput. Figure 3.25 shows a working

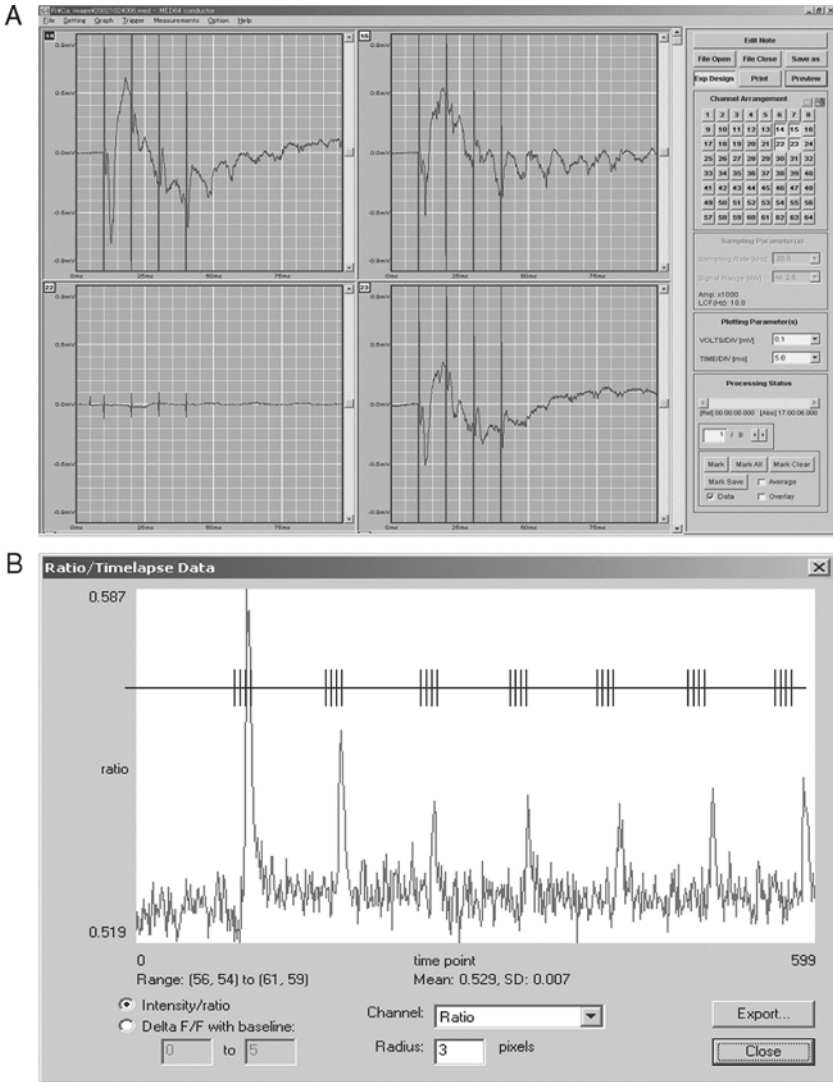


FIGURE 3.24. Simultaneous multi-cellular calcium imaging and multi-site electrophysiological recording. (A) Field potential was recorded with MED64 System at 4 sites in the pyramidal layer of hippocampus slice culture during the burst stimulation. The traces show the responses to a single 4-pulse stimulation. (B) Fluorescence intensity was simultaneously measured in the same pyramidal layer of hippocampus slice culture during the burst stimulation using a 3i digital microscopy workstation. (Courtesy of Intelligent Imaging Innovations.)

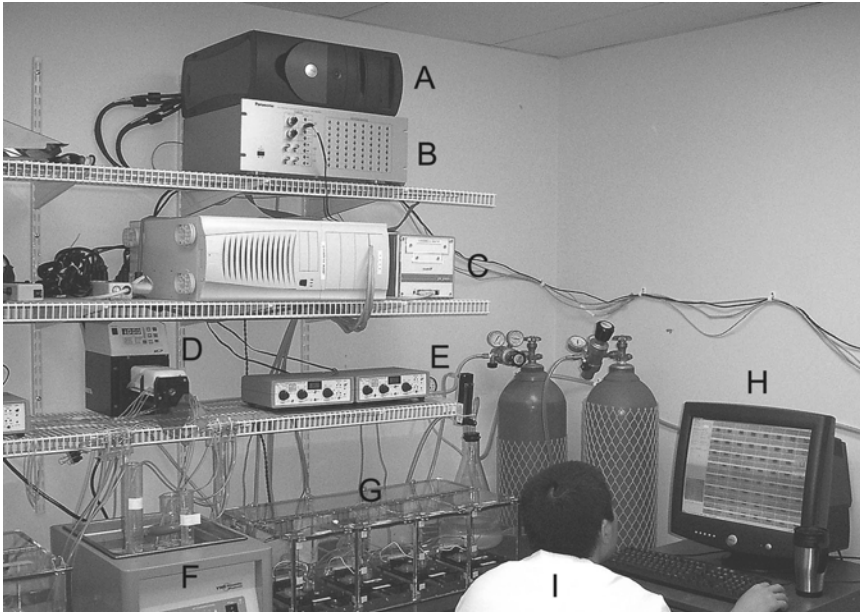


FIGURE 3.25. The DS-MED system for drug screening with MEAs. (A) A PC running the software that controls all the hardware and runs experiments. (B) A Panasonic MED64 Amplifier. (C) Custom multiplexing hardware that enables running multiple interleaved experiments in parallel. (D) An eight-line pump for perfusion. (E) Two inline heaters that handle two lines each. (F) A water bath containing ACSF and test compounds. (G) A custom four-chamber incubator with four MEAs running independent experiments. (H) A computer display showing the control software. (I) Lab technician Frank Tsuji. (Courtesy Tensor Biosciences.)

prototype capable of running four MEA experiments in parallel. The custom hardware, labeled C in the figure, is a multiplexing system that enables a single MED64 amplifier to run multiple interleaved experiments, each with its own MEA and automatic stimulation electrode switching (no patch cables). The custom software, shown at H, controls all the experiments from a single interface, and allows each one to start and stop independently, which is key to optimizing throughput because anytime a slice goes bad it can be replaced, which would not be possible with batch processing. The custom incubator, labeled G, lets the operator access any of four MEAs quickly and easily without leaving her chair.

Looking beyond enhanced traditional experiments for safety testing, the use of MEA technology for drug discovery purposes can also serve the need for more realistic information-rich tissue models in drug discovery. Currently most neurobiological drug discovery programs jump from single-cell screening to whole-animal behavioral testing. In so doing they skip the network level of analysis, that is, the analysis of drug effects on intact networks of neurons. Behavior is the product of networks, not single neurons. Single-cell studies, though extremely

useful for initial screening, are ultimately lacking in realism and relevance. And behavioral studies, though invaluable for safety testing, rely on indirect measures of physiological activity that are subject to a great deal of interpretation in the context of treatment quality evaluation.

A more ideal approach would appear to be the use of *in vivo* multi-electrodes in combination with behavioral experiments. Here drug effects observed on a network-level activity can be correlated with behavioral effects in real-time. However, this approach has very limited throughput. One of the more exciting potential uses for MEAs is to employ them as higher-throughput versions of these experiments. By focusing on the replication of desirable physiological effects established with the multi-electrode *in vivo* method, and then parallelizing testing with hardware such as the DS-MED, higher-throughput network-level drug testing might become a reality.

## References

- Buzsaki, G., and Chrobak, J.J. (1995). Temporal structure in spatially organized neuronal ensembles: A role for interneuronal networks. *Curr. Opin. Neurobiol.* 5: 504–510.
- Chen, S.C. and Wu, F.S. (2004). Mechanism underlying inhibition of the capsaicin receptor-mediated current by pregnenolone sulfate in rat dorsal root ganglion neurons. *Brain Res.* 1027: 196–200.
- Darbon, P., Yvon, C., Legrand, J.C., and Streit, J. (2004). LNaP underlies intrinsic spiking and rhythm generation in networks of cultured rat spinal cord neurons. *Eur. J. Neurosci.* 20: 976–988.
- Egashira, K., Nishii, K., Nakamura, K., Kumai, M., Morimoto, S., and Shibata, Y. (2004). Conduction abnormality in gap junction protein connexin45-deficient embryonic stem cell-derived cardiac myocytes. *Anat. Rec.* 280A: 973–979.
- Egert, U., Schlosshauer, B., Fennrich, S., Nisch, W., Fejtli, M., Knott, T., Mueller, T., and Haemmerle, H. (1998). A novel organotypic long-term culture of the rat hippocampus on substrate-integrated multielectrode arrays. *Brain Res. Prot.* 2: 229–242.
- Eichenbaum, H. (1997). How does the brain organize memories? *Science* 277: 330–332.
- Feld, Y., Melamed-Frank, M., Kehat, I., Tal, D., Marom, S., and Gepstein, L. (2002). Electrophysiological modulation of cardiomyocytic tissue by transfected fibroblasts expressing potassium channels: A novel strategy to manipulate excitability. *Circulation* 105: 522–529.
- Gross, G.W. (1979). Simultaneous single unit recording *in vitro* with a photoetched laser deinsulated gold multimicroelectrode surface. *IEEE Trans. Biomed. Eng.* 26: 273–278.
- Gross, G.W., Rieske, E., Kreutzberg, G.W., and Meyer, A. (1977). A new fixed-array multimicroelectrode system designed for long-term monitoring of extracellular single unit neuronal activity *in vitro*. *Neurosci. Lett.* 6: 101–106.
- Honma, S., Shirakawa, T., Katsuno, Y., Namihira, M., and Honma, K. (1998). Circadian periods of single suprachiasmatic neurons in rats. *Neurosci. Lett.* 250: 157–160.
- Jarrard, L.E. (1993). On the role of the hippocampus in learning and memory in the rat. *Behav. Neural. Biol.* 60: 9–26.
- Jimbo, Y., Robinson, H.P.C., and Kawana, A. (1993). Simultaneous measurement of intracellular calcium and electrical activity from patterned neural networks in culture. *IEEE Trans. Biomed. Eng.* 40: 804–810.

- Jimbo, Y., Robinson, H.P.C., and Kawana, A. (1998). Strengthening of synchronized activity by tetanic stimulation in cortical cultures: Application of planar electrode arrays. *IEEE Trans. Biomed. Eng.* 45: 1297–1304.
- Jobling, D.T., Smith, J.B., and Wheal, H.V. (1981). Active microelectrode array to record from the mammalian central nervous system *in vitro*. *Med. Biol. Eng. Comput.* 19: 553–560.
- Legrand, J.C., Darbon, P., and Streit, J. (2004). Contributions of NMDA receptors to network recruitment and rhythm generation in spinal cord cultures. *Eur. J. Neurosci.* 19: 521–532.
- Lisman, J.E. (1999). Relating hippocampal circuitry to function: Recall of memory sequences by reciprocal dentate-CA3 interactions. *Neuron.* 22: 233–242.
- Lu, Z.J., Pereverzev, A., Liu, H.L., Weiergräber, M., Henry, M., Krieger, A., Smyth, N., Hescheler, J., and Schneider, T. (2004). Arrhythmia in isolated prenatal hearts after ablation of the Cav2.3 ( $\alpha 1E$ ) subunit of voltage-gated Ca<sup>2+</sup> channels. *Cell Physiol. Biochem.* 14: 11–22.
- Marr, D. (1971). Simple memory: A theory for archicortex. *Proc. R. Soc. Lond. B Biol. Sci.* 272: 23–81.
- McNaughton, N. and Morris, R. G. (1987). Hippocampal synaptic enhancement and information. *Trends Neurosci.* 10: 408–415.
- Muller, R. (1996). A quarter of a century of place cells. *Neuron* 17: 813–822.
- Nadel, L. and Moscovitch, M. (1997). Memory consolidation, retrograde amnesia and the hippocampal complex. *Curr. Opin. Neurobiol.* 7: 217–227.
- Nicholson, C. and Freeman, J.A. (1975). Theory of current source-density analysis and determination of conductivity tensor for anuran cerebellum. *J Neurophysiol* 38: 356–368.
- Nicholson, C. and Llinas, R. (1975). Real time current source-density analysis using multi-electrode array in cat cerebellum. *Brain Res.* 100: 418–424.
- Novak, J.L. and Wheeler, B.C. (1988). Multisite hippocampal slice recording and stimulation using a 32 element microelectrode array. *J. Neurosci. Meth.* 23: 149–159.
- Oka, H., Shimono, K., Ogawa, R., Sugihara, H., and Taketani, M. (1999). A new planar multielectrode array for extracellular recording: Application to hippocampal acute slice. *J. Neurosci. Meth.* 93: 61–67.
- O’Keefe, J. and Recce, M.L. (1993). Phase relationship between hippocampal place units and the EEG theta rhythm. *Hippocampus* 3: 317–330.
- Paulsen, O. (2003). Network oscillations studied using planar multielectrode arrays. *The Second Network Physiology Symposium, satellite symposium of The Society for Neurosciences 33rd Annual Meeting, New Orleans, Louisiana, USA.*
- Ren, D. and Miller, J.D. (2003). Primary cell culture of suprachiasmatic nucleus. *Brain Res. Bull.* 61: 547–553.
- Shimono, K., Brucher, F., Granger, R., Lynch, G., and Taketani, M. (2000). Origins and distribution of cholinergically induced beta rhythms in hippocampal slices. *J. Neurosci.* 20: 8462–8473.
- Shimono, K., Kubota, D., Brucher, F., Taketani, M., and Lynch, G. (2002). Asymmetrical distribution of the Schaffer projections within the apical dendrites of hippocampal field CA1. *Brain Res.* 950: 279–287.
- Squire, L.R. and Zola, S.M. (1998). Episodic memory, semantic memory, and amnesia. *Hippocampus* 8: 205–211.
- Streit, J., Tschertner, A., Heuschkel, M.O., and Renaud, P. (2001). The generation of rhythmic activity in dissociated cultures of rat spinal cord. *Eur. J. Neurosci.* 14: 191–202.

- Thomas, Jr, C.A., Springer, P.A., Loeb, G.E., Berwald-Netter, Y., and Okun, L.M. (1972). A miniature microelectrode array to monitor the bioelectric activity of cultured cells. *Exp. Cell. Res.* 74: 61–66.
- Treves, A. and Rolls, E.T. (1992). Computational constraints suggest the need for two distinct input systems to the hippocampal CA3 network. *Hippocampus* 2: 189–199.
- Tscherter, A., Heuschkel, M.O., Renaud, P., and Streit, J. (2001). Spatiotemporal characterization of rhythmic activity in rat spinal cord slice cultures. *Eur. J. Neurosci.* 14: 179–190.
- Tulving, E., and Markowitsch, H.J. (1998). Episodic and declarative memory: Role of the hippocampus. *Hippocampus* 8: 198–204.
- Welsh, D.K., Logothetis, D.E., Meister, M., and Reppert, S.M. (1995). Individual neurons dissociated from rat suprachiasmatic nucleus express independently phased circadian firing rhythms. *Neuron* 14: 697–706.